

## Article

# Expression, Purification and Characterization of a Novel Rusticyanin from the Psychrotolerant *Acidithiobacillus ferrivorans*

Yuandong Liu \*, Lixiang Chen , Xiangdong Shangguan, Jingying Ouyang, Jiayu He, Kan Wang, Yan Tong, Runlan Yu, Weimin Zeng, Xueling Wu, Li Shen and Guanzhou Qiu

Key Laboratory of Biohydrometallurgy of Ministry of Education, School of Minerals Processing and Bioengineering, Central South University, Changsha 410083, China; lixche@126.com (L.C.); xiangdongsg@sina.cn (X.S.); jingyoy@yeah.net (J.O.); jiayuhe3328@126.com (J.H.); dlwqw126@126.com (K.W.); qq3461567793@163.com (Y.T.); yrl715@sina.com (R.Y.); zengweimin1024@126.com (W.Z.); wxlcsu@csu.edu.cn (X.W.); lishen@csu.edu.cn (L.S.); gzhqiu@sina.cn (G.Q.)

\* Correspondence: yuandong\_liu@csu.edu.cn; Tel.: +86-731-88877472

**Abstract:** Rusticyanin plays a crucial role in ferrous oxidation of sulfide minerals during bioleaching for industrial metal extraction. Diverse isoforms of rusticyanin have been found, but until now, except for type-A rusticyanin, other isoforms or sources of rusticyanin have been scarcely investigated. Here, a rusticyanin (gene locus 0470) from the psychrophilic *Acidithiobacillus ferrivorans* was gene-cloned, expressed, purified, and assembled in vitro. All forms of the protein exhibit extreme acid stability, even at pH 0.3. The stability of the protein is obviously enhanced after binding of the copper cofactor; the oxidation state is more stable than the reduced state. The protein has characteristic UV-vis peaks and EPR signals similar to type-A or type-B rusticyanin but is different with a small position shift and an obvious intensity change. The vibrational spectrum of the apoprotein was more different than these between the oxidation and reduced states of the protein. The ferrous oxidation kinetic rate constant of the protein is obviously faster than that of both the type-A and type-B rusticyanins previously reported. Further bioinformatics analysis reveal their changes in sequence and molecule: the mutations related to the peculiar shield belt mostly account for the variation in the properties of the protein, and the classification of the protein as a new isoform, type-C rusticyanin, is proposed.

**Keywords:** rusticyanin; isoform; *Acidithiobacillus ferrivorans*; overexpression; characterization; kinetic rate constant



**Citation:** Liu, Y.; Chen, L.; Shangguan, X.; Ouyang, J.; He, J.; Wang, K.; Tong, Y.; Yu, R.; Zeng, W.; Wu, X.; et al. Expression, Purification and Characterization of a Novel Rusticyanin from the Psychrotolerant *Acidithiobacillus ferrivorans*. *Separations* **2023**, *10*, 448. <https://doi.org/10.3390/separations10080448>

Academic Editor: Ki Hyun Kim

Received: 30 June 2023

Revised: 29 July 2023

Accepted: 8 August 2023

Published: 13 August 2023



**Copyright:** © 2023 by the authors. Licensee MDPI, Basel, Switzerland. This article is an open access article distributed under the terms and conditions of the Creative Commons Attribution (CC BY) license (<https://creativecommons.org/licenses/by/4.0/>).

## 1. Introduction

Rusticyanin belongs to the type I copper protein of the cupredoxin family and is the only known enzyme in copper-related proteins to exhibit both extreme acid stability and high redox potential [1]; it also plays a crucial role in ferrous oxidation of the iron-oxidizing bacteria *Acidithiobacillus*, which constitutes one of the core mechanisms of mineral bioleaching for industrial metal extraction [2,3]. Rusticyanin was initially found in the mesophilic acidophilic chemolithotrophic *Acidithiobacillus ferrooxidans* and made up to 5% of the total proteins in the cell under energy sources with ferrous ions or iron-containing minerals [4]. The gene for rusticyanin was first cloned from *A. ferrooxidans* ATCC 23270 [5]. Then, it was shown to be situated in a gene cluster of the *rus* operon, where a periplasmic dihemic cytochrome  $c_4$  of *Cyc1* (*cyc1*), an outer membrane high molecular weight cytochrome *c* of *Cyc2* (*cyc2*), an unknown function of ORF (*orf*), an aa3-type cytochrome oxidase (*coxBACD*) and the periplasmic rusticyanin (*rus*) were encoded sequentially [6]. Based on studies in operon organization, subcellular localization, and transcriptional regulation, a model for the respiratory electron transport chain of ferrous oxidation was proposed:  $\text{Fe}^{2+} \rightarrow \text{Cyc2} \rightarrow \text{rusticyanin} \rightarrow \text{Cyc1} \rightarrow \text{cytochrome oxidase} \rightarrow \text{O}_2$  [2,6]. Rusticyanin encoded by the *rus* operon has been studied very well; many properties have

been characterized [1,4,5,7–9], and lots of structures have also been determined [1,9]. Moreover, rusticyanin can be efficient in anticancer [10] and antimalarial [11] therapies. A conventional biosupercapacitor built from rusticyanin was also reported [12].

However, rusticyanin exhibits some diversity. In the beginning, multiple copies of the gene (*rus*) for rusticyanin were further found to be present in the genomes of some strains of *A. ferrooxidans* [13]. Based on sequence differences and gene context background, these rusticyanin genes can be distinctly classified into two forms [13]. The more common form was located in the *rus* operon and found to be present in all studied strains till now, including those harboring only a single copy of the gene, such as the strains of ATCC 23270, and their protein was designated as type-A rusticyanin. The less common form was designated as type-B rusticyanin, which occurred in strains harboring multiple copies of the gene and exhibited a totally different genetic background from the *rus* operon gene cluster [13,14]. Both forms of these rusticyanins from *A. ferrooxidans* were highly conserved, with >98% identities in each form, though there was <81% identities between the two forms [13]. The kinetic rate constants of ferrous oxidation for type-B from *A. ferrooxidans* JCM3865 and type-A from *A. ferrooxidans* ATCC23270 were measured, and the results showed that type-B reacted with ferrous ions more slowly than type-A [14]. Afterwards, rusticyanins were also found in psychrotolerant *Acidithiobacillus ferrivorans*, and the remaining rusticyanins in them, except for type-A, may be considered as mechanisms for adaptation to low temperatures [15,16]. Meanwhile, rusticyanin has also been detected in the genomes of other acidophilic bacteria, e.g., iron-oxidizing *Acidithiobacillus spp.* and *Sulfobacillus spp.* [17–19]. Some of these bacteria do not appear to possess the *rus* operon, and so their iron oxidation is thought to proceed by another, as yet not fully elucidated, mechanism [17–19]. Unfortunately, almost all of our knowledge of rusticyanin so far is limited to the research on type-A rusticyanin from *A. ferrooxidans* [1,2,4–12] as other isoforms or sources of rusticyanins are scarcely investigated. So it is very necessary to explore the new diversity of rusticyanin, investigate each isoform, and compare them to gain a full understanding of rusticyanins, especially considering their important roles, peculiar properties, and potential applications [1,4,7–12].

*A. ferrivorans* is a psychrotolerant iron- and sulfur-oxidizing chemolithotrophic acidophile that shares the same *Acidithiobacillus* genus as *A. ferrooxidans* but differs in cell motility, tolerance to low temperatures, and responses to pH [17]. The whole genome of *A. ferrivorans* SS3 has been sequenced and annotated, and three genes (locus 0470, 1864, and 1718) of rusticyanin were also found to be present in that genome (Table S2) [17], which facilitates bioinformatics comparative analysis for rusticyanins from *A. ferrivorans* SS3 and various sources (Figures S1 and S2). The gene at locus 1864 is situated in a gene context of conserved *rus* operons and also has a conserved sequence with the type-A rusticyanin from *A. ferrooxidans*, so it is evidently related to type-A. The gene at locus 1718 has a highly conserved amino acid sequence (near 96%) with the type-B rusticyanin from *A. ferrooxidans*, so it should correspond to type-B. However, the rusticyanin of the gene locus 0470 exhibits a distinct sequence, which is neither related to type-A nor type-B rusticyanins from *A. ferrooxidans*, so it is difficult to be designated. Friendly environmental hydrometallurgy at low temperatures is principally promoted by *A. ferrivorans*, and its bioleaching mechanism has recently attracted particular attention [15–17]. So it is of great interest to investigate the potential application significance of rusticyanins from the psychrophilic *A. ferrivorans*.

In this study, the rusticyanin encoded by the gene at locus 0470 from *A. ferrivorans* SS3 was overexpressed in *E. coli*, purified using one-step affinity chromatography, and assembled with copper in vitro. The properties of apo-, oxidized, and reduced forms of the recombinant protein were investigated systematically. This protein exhibited some basic properties akin to the previously reported rusticyanins but was different in intensity changes, particularly in the more extreme acid stability and the surprising faster electron transfer rate from ferrous ions. Further bioinformatics analysis revealed the essential molecular reasons contributing to their property differences, and the classification of the

protein as a new isoform, type-C rusticyanin, is proposed. The existence of this new isoform rusticyanin with high ferrous oxidation efficiency facilitates the growth of the psychrophilic *A. ferrivorans* in cold environments.

## 2. Materials and Methods

### 2.1. Cloning, Expression, and Purification of the Recombinant Type-C Rusticyanin from *A. ferrivorans*

*A. ferrivorans* SS3 was kindly obtained from Prof. Mark Dopson (Linnaeus University, Sweden) [17]. This bacterium was cultured in 9 K medium that contained 3.0 g  $(\text{NH}_4)_2\text{SO}_4$ , 0.1 g KCl, 0.5 g  $\text{K}_2\text{HPO}_4$ , 0.5 g  $\text{MgSO}_4 \cdot 7\text{H}_2\text{O}$ , and 0.01 g  $\text{Ca}(\text{NO}_3)_2$  per liter, supplemented with 44.7 g/L of ferrous sulfate. The initial pH values of these media were adjusted to 2.0 with  $\text{H}_2\text{SO}_4$  and were then filter sterilized before the addition of ferrous sulfate. The cultures of the bacterium were grown in 500 mL flasks containing 300 mL medium under aerobic conditions (170 rpm) at 22 °C. When bacterium cells entered the logarithmic growth phase, cells were harvested at a later logarithmic phase of cell growth via centrifugation at 4 °C for 10 min at 12,000 rpm using a 5804R centrifuge (Eppendorf, Wesbury, NY, USA). The supernatant was discarded, and pelleted cells were immediately processed for DNA extraction using the PureLink™ Genomic DNA Kit (Invitrogen Corp., Carlsbad, CA, USA) and then used as a template for polymerase chain reaction (PCR) for amplification of the sequence area containing the type-C rusticyanin gene (locus at 0470). Specific primers were designed according to the whole genome sequence of *A. ferrivorans* SS3 using the Primer Premier 5.0 software (Text S1). PCR amplification was performed using Taq DNA polymerase, and samples were subjected to 30 cycles of 45 s of denaturation at 95 °C, 45 s of annealing at 54 °C, and 1 min of elongation at 72 °C in a T100 Thermal Cycler (Bio-Rad Laboratories Inc., Hercules, CA, USA). The resulting PCR product was gel purified using the UltraClean 15 DNA Purification Kit (MO BIO Laboratories, Inc., Carlsbad, CA, USA), then used as a template for further PCR for amplification of the target sequence of the type-C gene. The forward primer (RusC-F) was 5'-GATATACATATGCATCATCACCACCACGGCACCCCACTGGACACCTCCTGG-3', containing a NdeI site (CATATG), codons for the amino acid sequence MHHHHHHHG (start codon and hexahistag), and codons for amino acids 1–7 of the mature type-C rusticyanin. The reverse primer (RusC-R) was 5'-GGCCGCAAGCTTCTATTTTACAACGATCTTGCCG AACATGC-3', containing a HindIII site (AAGCTT), a stop anticodon, and anticodons for the last eight amino acids of type-C. PCR amplification was performed using AC-CUZYME™ DNA polymerase (Biolone Reagents Ltd., London, UK) in the T100 Thermal Cycler. The resulting PCR product was gel purified and ligated into a *pET-30a* expression vector, resulting in the *pET-30a::RusC* plasmid, and then transformed into *E. coli* strain BL21 competent cells for expression purposes. The plasmid isolated from the expression strain was first digested with *NdeI* and *HindIII*, checked via agarose gel electrophoresis analysis for successful ligation, and further confirmed using custom sequencing for the correct sequence.

The *E. coli* BL21 with the *pET-30a::RusC* plasmid was grown at 37 °C with 220 rpm shaking in an LB medium containing kanamycin (50 mg/L). When the culture reached an  $\text{OD}_{600}$  of 1.0, the cells were induced with 150  $\mu\text{M}$  isopropyl  $\beta$ -D-1-thiogalactopyranoside (IPTG) for 16 h at 15 °C with 220 rpm shaking for the overexpression of the protein.

The cells were harvested through centrifugation, resuspended in a 50 mM phosphate pH 8.0 buffer containing 500 mM NaCl and 10 mM imidazole, and lysed with sonication (Autotune Series High Intensity Ultrasonic Sonicator, Scientz, Ningbo, Zhejiang, China). Cell debris was removed via centrifugation at  $39,000 \times g$  for 30 min at 4 °C. The supernatant was loaded on a HiTrap chelating nickel affinity column (GE Healthcare, Chicago, IL, USA) and washed with 50 column volumes of 50 mM phosphate pH 8.0 buffer containing 500 mM NaCl and 20 mM imidazole, and then eluted with a linear gradient from 30 to 300 mM imidazole over ten column volumes. Protein purity was analyzed via sodium dodecyl sulfate-polyacrylamide gel electrophoresis (SDS-PAGE) stained with Coomassie Blue [20].

## 2.2. Assembly of the Holo-Rusticyanin and Preparations for the Oxidized and Reduced States

Pure protein fractions were pooled and dialyzed overnight against the 2 L solution of HCl pH 2.0, and repeated twice with each dialysis lasting 2 h to remove excess other impurities. The purified protein lacked copper and corresponded to apo-rusticyanin. The apoprotein was incubated with an excess of copper chloride at 4 °C for 60 min to realize the assembly of the holoprotein, and then dialyzed at 4 °C for 3 h against a 2 L solution of HCl pH 2.0 repeatedly for three times to remove excess copper chloride. The obtained holoprotein was first in the oxidized state with Cu(II). The reduced rusticyanin with Cu(I) was prepared by reacting with an excess of ferrous chloride for 1 h followed by anaerobically dialysis at 4 °C for 3 h against a 2 L solution of HCl pH 2.0, repeated three times, to remove the excess reducing agent. The oxidized rusticyanin with Cu(II) was prepared by reacting with an excess of Na<sub>2</sub>IrCl<sub>6</sub> or dithionite for 1 h according to the previous report [13], followed by dialysis at 4 °C for 3 h against a 2 L solution of HCl pH 2.0, repeated three times, to remove the excess oxidizing agent. The desired concentrations of the protein were achieved via ultrafiltration in an Amicon 1.5 K molecular weight cutoff spin concentrator (Millipore). The concentrations of the protein were determined through optical absorption at 280 nm according to its extinction coefficient [4,7,13], or using the Bradford method with bovine serum albumin as the standard.

## 2.3. Characterization Methods

The properties of the apo-, oxidized, and reduced forms of the recombinant type-C were investigated using calorimetry and various spectral methods. The molecular mass of the assembled holoprotein was determined using an UltrafleXtreme TOF/TOF spectrometer (Bruker Daltonics, Billerica, MA, USA). Differential scanning calorimetry (DSC) observations for the apo-, oxidized, and reduced forms of the protein were taken with a DSC 214 polima Differential Scanning Calorimeter equipped with the Proteus<sup>®</sup> software (NETZSCH-Gerätebau GmbH, Selb, Germany). The freeze-dried protein samples were placed in an aluminum pan crucible, hermetically closed with a lid and placed in an DSC furnace. An empty aluminum pan was used as a reference. Heating was conducted with a 1 min equilibration at 10 °C, followed by heating at 10 °C/min to 200 °C with nitrogen as a purge gas. The average endothermic heat flow was calculated from the three protein samples using the Proteus<sup>®</sup> 8.9 software.

The matrix assisted laser desorption/ionization time-of-flight mass spectrometry (MALDI-TOF-MS) result was obtained in a linear positive mode from  $m/z$  2500–20,000 using  $\alpha$ -cyano-4-hydroxy-cinnamic acid (saturated solution in 50% acetonitrile with 0.1% trifluoroacetic acid) as the ultraviolet (UV)-absorbing matrix. UV-visible scanning spectra were carried out on a Techcomp UV-2300 spectrophotometer. X-band electronic paramagnetic resonance (EPR) spectra were recorded at 100 K on a JEOL JES-FE1XG spectrometer. Parameters for recording the EPR spectra were typically 15–30 mT/min sweep rate, 0.63 mT modulation amplitude, 9.14 GHz frequency, and 4 mW incident microwave power; sweep time was 2 min. Fourier transform infrared (FTIR) spectroscopy was performed on a NEXUS 670 FTIR Spectrometer (Thermo Nicolet, Madison, WI, USA) after the protein samples were freeze-dried into solids.

## 2.4. Kinetic Measurement between the Oxidized Rusticyanin and Ferrous ion

The kinetic experiment was performed on an Epoch Microplate Spectrophotometer equipped with the control, data collection, and analysis software of Gen5 (BioTek Instruments, Inc., Winooski, VT, USA). The kinetic mode procedure using the absorbance detection method on endpoints or kinetics read types with pathlength correction was selected. The absorbance at 600 nm of the oxidized rusticyanin was used as a spectrophotometric probe to monitor the reactions. The oxidized rusticyanin and the ferrous ion were all prepared in identical degassed solutions of HCl pH 2.0. Microplate-based reactions were performed in a total volume of 200  $\mu$ L consisting 100  $\mu$ L of the protein solution, and initiated by rapidly mixing 100  $\mu$ L of ferrous ion solution. The concentration of the oxidized

rusticyanin in the reaction system was initially 0.25 mM, and the concentrations of ferrous ions were initially at 7, 10, 15, 25 and 50 mM, respectively. The concentrations of ferrous ion were in 100-fold or greater excess than those of the protein, ensuring pseudo-first-order conditions and allowing the concentrations of ferrous ions to be treated as constants during the experiments. Kinetic measurements were typically performed by reading every 2 s for 10 min. Each electron-transfer reaction was permitted to proceed to between 95% and 98% completion. All temperatures were maintained at 25 °C. The kinetic measurement adopts the pseudo-first-order rate method [14].

### 2.5. Bioinformatics Analysis

For bioinformatics analysis, the following websites or tools were used: NCBI (National Center for Biotechnology Information) database BLAST ([www.ncbi.nlm.nih.gov/blast/](http://www.ncbi.nlm.nih.gov/blast/) (accessed on 30 June 2023)) for similarity search; SignalP ([www.cbs.dtu.dk/services/SignalP/](http://www.cbs.dtu.dk/services/SignalP/) (accessed on 30 June 2023)) for signal peptide prediction; Cluster X 1.83 for sequence alignment and phylogenetic analysis; and the Compute pI/Mw tool from the Swiss Institute of Bioinformatics for theoretical molecular mass calculation. All molecular modeling and structure analysis were performed on Discover Studio (Accelrys Inc., San Diego, CA, USA). The structure of a type-A rusticyanin of *A. ferrooxidans* from the Protein Data Bank (PDB) of RCSB (PDB number 1CUR) was selected as the template. The initial apoprotein 3D structure of the rusticyanin was built using the Modeler program. The copper prosthetic group was further added to it to manually form the holoprotein model. Then, the holoprotein model was encompassed with a 2 nm layer of water molecules to be optimized through a series of molecular simulation procedures. The final model was passed through the assessments of ProStat and Profile3D.

## 3. Results and Discussion

### 3.1. Gene Cloning, Protein Purification, and Assembly of Type-C Rusticyanin from *A. ferrivorans*

The type-C rusticyanin gene was successfully amplified using PCR in two steps from the genomic DNA of *A. ferrivorans* SS3, and finally ligated into the expression vector, as confirmed with enzyme-digested agarose gel electrophoresis analysis (Figure 1a). The constructed *pET-30a::RusC* plasmid was further verified using DNA sequencing and shown to be completely correct. PCR techniques were used to successfully add a six-His-tag to the N-terminal of the protein, which enabled to adopt the one-step affinity chromatography and greatly accelerated the protein purification process.

The expression of (the x) type-C in *E. coli* BL21(DE3) was carried out at different temperatures and IPTG concentrations, and proteins were obtained at all tested conditions. It was found that the protein expressed better at a 0.6 mM IPTG concentration and resulted in more soluble protein at a cold temperature (15 °C) than at 37 °C. The purification of type-C was performed on a nickel affinity column with loading buffer containing different imidazole concentrations. It was found that the addition of imidazole to a loading buffer can suppress the adsorption of non-specific proteins and improve the purification of type-C, and a minimum concentration of 20 mM imidazole is enough for high-quality purification of the protein. The final protein yield after purification was 7.0%, which is comparable with that of the recombinant rusticyanins from *A. ferrooxidans* [14,21], and the results also suggest that the T7 polymerase promoter/BL21(DE3) expression system is an ideal system for expressing the rusticyanin protein from psychrotolerant *A. ferrivorans* in high yield; the hexahistag in the N-terminal and chelating nickel affinity separation technique are responsible for the efficient purification of the protein.

The purity of the purified protein was examined using SDS-PAGE, and single bands corresponding to 17.5 kDa were observed with >95% purity (Figure 1b), which was in agreement with the deduced molecular mass of a monomer. The protein eluted from the nickel column was observed to be a clear color, indicating a lack of the copper cofactor and corresponding to the apoprotein of type-C (Figure 1c). The protein incubated with copper chloride remained in a deep blue color after dialysis, indicating it had successfully

bound to the copper cofactor and formed the holoprotein (Figure 1c). The oxidized type-C rusticyanin displayed a deep blue color, but the reduced version showed a clear color (Figure 1c).

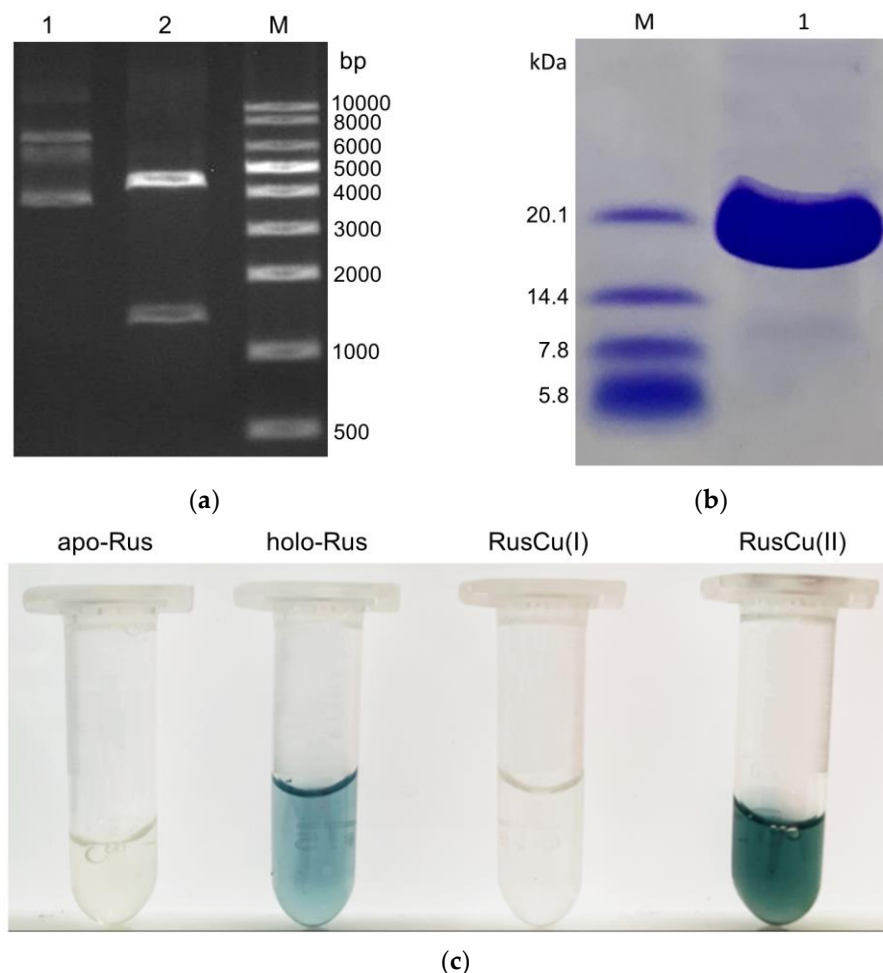


**Figure 1.** Cloning, expression, and purification of the type-C rusticyanin from *A. ferrivorans*. (a) Agarose gel electrophoresis analysis. Lane 1, the constructed *pET-30a::RusC* plasmid, has three bands from bottom to top: the superhelical, relaxed and linear fractures of the plasmid, respectively. Lane 2, the plasmid digested with *NdeI* and *HindIII* endonucleases, has two bands from bottom to top corresponding to the target gene and the remaining plasmid, respectively. The target gene band position is well in line with the length of the digested sequence containing the type-C gene. Lane M, nucleic acid length mark; (b) Coomassie blue-stained SDS-PAGE analysis. Lane M, molecular mass standards; lane 1, the purified type-C rusticyanin; (c) colors of the type-C rusticyanin under different forms or states. From left to right: apo-Rus, the purified protein after nickel column elution; holo-Rus, the protein assembled from the apo-Rus with cupric ion; RusCu(I), the oxidized state of the protein; RusCu(II), the reduced state of the protein.

All the apoproteins, including the oxidized and reduced states of the type-C rusticyanin, exhibited extreme acid stability, and could be stored in a solution of HCl pH 2.0 at 4 °C for at least 4 months without appreciable deleterious or air-oxidized effects. The theoretical isoelectric point of type-C is 9.14. The high concentration of the protein will produce precipitates when kept or dialyzed in a phosphate pH 8.0 solution overnight or when kept in a more alkaline solution for a longer time, but the precipitates can be quickly restored or dissolved when put into a HCl pH 2.0 solution again. Previous reports had revealed that rusticyanin (type-A) had stable activity in pH 1–3 [1,4]. By contrast, the

type-C in apo-, oxidized, and reduced forms exhibited more acid stability even when pH values were lower than 0.3.

### 3.2. MALDI-TOF-MS and DSC of the Type-C Rusticyanin

The MALDI-TOF-MS of the assembled holoprotein demonstrates a large peak at 17,575.52 Da (Figure 2a), which is rightly in agreement with the theoretical average molecular mass of the type-C rusticyanin with the His-tags in the N-terminal plus the Cu prothetic group. During the MALDI-MS process, protein samples have to mixed with acids and undergo strong laser high temperature vaporization desorption, which can easily lead to the disruptions of their labile cofactors or prothetic groups. An example from our research is that the MALDI-TOF-MS of the Iro protein showed two peaks corresponding to the holoprotein and apoprotein, respectively, due to its acid-labile  $[\text{Fe}_4\text{S}_4]$  [22]. However, there is no mass peak at the site corresponding to the apoprotein in the MALDI-TOF-MS, which indicates that the holoprotein binds the copper prothetic group very firmly and the copper does not get lost even after a vicious MS process. The result is also in line with the extreme acid stability behavior of the type-C rusticyanin.

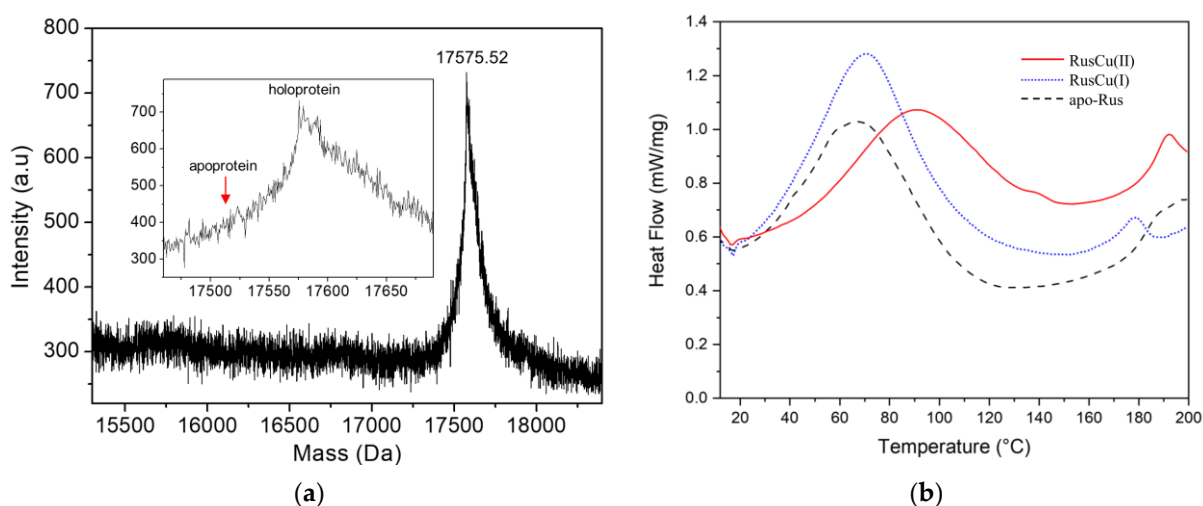


**Figure 2.** Characterizations of the type-C rusticyanin from *A. ferrivorans*. (a) MALDI-TOF-MS of the assembled holoprotein: the inset shows the local details around the mass peak of the holoprotein; (b) DSC for the apo-, oxidized, and reduced forms of the type-C rusticyanin.

DSC is a well-established technique for protein stability studies [23,24]. To further investigate the stability of the type-C rusticyanin, calorimetric observations in the temperature range from 10 °C to 200 °C for the apo-, oxidized and reduced forms of the type-C rusticyanin samples were taken (Figure 2b). All DSC curves of these forms contain two major endothermic peaks. One is below 150 °C, which mainly results from the thermal denaturation of the protein since the previously reported ovalbumin, lysozyme, myoglobin, and fibrinogen also showed similar endothermic peaks of the thermal denaturation in this area [25–29]. Another is above 150 °C, which should be related to the thermal decomposition of the protein because the previously reported thermal oxidation is also in this temperature range. However, the DSC curves of each form of type-C exhibit obvious differences in details. For the thermal denaturation temperature, the holoprotein is higher than the apoprotein, and the oxidized form is higher than the reduced form. The thermal denaturation transition temperatures of the apo-, reduced, and oxidized forms of the type-C are 66.6 °C, 71.2 °C and 90.8 °C, respectively. The thermal denaturation endothermic width or calorimetric enthalpy of the holoprotein, reduced or oxidized form is obviously broader or higher than that of the apoform. These results further indicate that the holoprotein is more stable than the apoprotein, which is in good agreement with the MALDI-TOF-MS results. Moreover, a minor endothermic peak occurs in the shoulder of

the thermal oxidation peak of the oxidized and reduced forms of type-C, which should be related to the copper binding because of the lack of it in the apoprotein. In other words, the copper ion provides type-C with an excess of thermodynamic stability compared with the apo form. However, the transition temperature of the minor peak of the oxidized type-C is higher than that of the reduced type C. Combining the thermal denaturation results, it can be concluded that the oxidized type-C is more stable than the reduced type C.

### 3.3. UV-Scanning and EPR of the Type-C Rusticyanin

The UV-visible spectrum of the oxidized type-C has a maximum absorbance around 600 nm and two minor absorbances around 450 and 750 nm, respectively, but that of the reduced type-C is absent and shows to be almost identical to that of the apoprotein (Figure 3a). The absorption at 600 nm, which is characteristic of type 1 copper sites, arises from a charge-transfer transition from S-Cys to copper. The band at 450 nm is observed for some other blue copper proteins; the band at 450 nm is also believed to be associated with a separate cysteine-copper charge-transfer transition. The type-A rusticyanin from *A. ferrooxidans* ATCC 23270 and the type-B rusticyanin from *A. ferrooxidans* JCM 3865 also showed similar absorbances, though there are differences among them in extinction coefficient [13]. The absorbance change between the oxidized and reduced states of the type-C is also completely consistent with that of the color change. Furthermore, though the type-C rusticyanin in the reduced state had no EPR activity, the protein in the oxidized state exhibited an EPR signal with g-values of 2.017, 2.2062 and 2.226 (Figure 3b), which is also akin to type-A and type-B [13], but different with some small position shifts and an obvious intensity change.

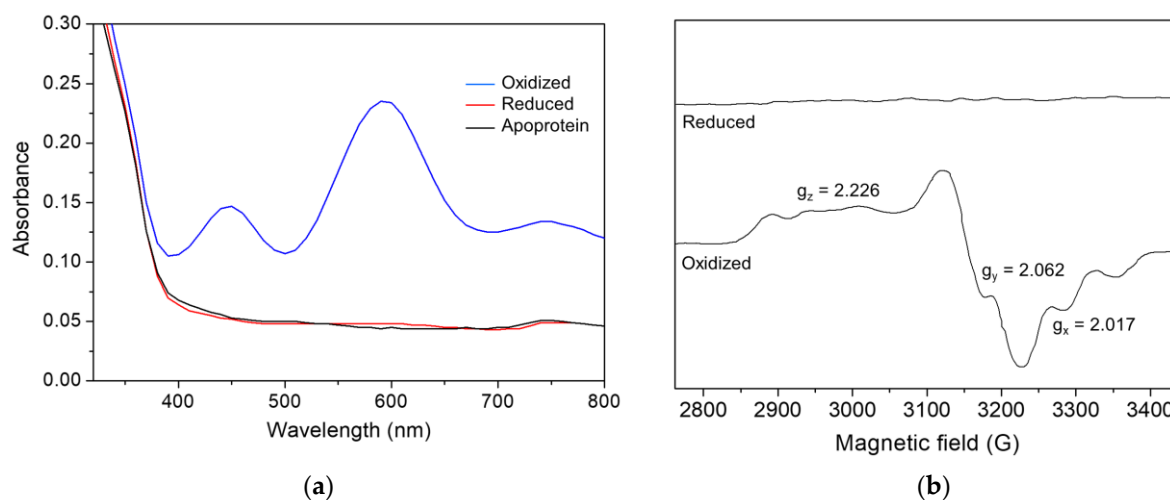


**Figure 3.** Characterizations of the type-C rusticyanin from *A. ferrovorans*. (a) UV-visible spectra of the type-C rusticyanin in apo-, oxidized, and reduced forms; (b) EPR spectra of the type-C rusticyanin in oxidized and reduced states.

### 3.4. FTIR for Apo-, Oxidized and Reduced States of the Type-C Rusticyanin

The FTIR spectra of the type-C rusticyanin have a series of typical vibrational absorbance bands, as described in the review of vibrational spectroscopy for proteins [22] (Figure 4). The regions around the peaks at 3289 and 3070  $\text{cm}^{-1}$  correspond to the amide A and B bands, respectively, which are responsible for the NH stretching vibrations of peptides. The region around the peak at 1643  $\text{cm}^{-1}$  is the amide I band, which is mainly from the C=O stretching vibration of peptides and can be used for protein secondary-structure analysis. The peaks at 1541  $\text{cm}^{-1}$  correspond to the amide II band, mainly from the out-of-phase combination of the NH inplane bend and the CN stretching vibration. The FTIR spectra of the type-C in apo-, oxidized, and reduced forms are highly identical in the amide I and II bands, indicating that neither the copper cofactor bound or unbound nor the switch

between the oxidized and reduced states hardly alter the secondary-structure conformation of the protein, which is well in line with previous reports [1,9]. Although the spectra of the protein in all forms are broadly identical, they differ in detail, showing changes in the relative intensities, especially for the apoprotein (Figure 4d). Firstly, a weak difference is present in the range from 2750 to 2150  $\text{cm}^{-1}$  for the apoprotein, where a turn is present around the site at 2600  $\text{cm}^{-1}$  corresponding to the sulfhydryl group of the only cysteine in the protein. Secondly, the most obvious difference is the range from 1450 to 400  $\text{cm}^{-1}$  for all the forms, but it is difficult to straightforwardly assign these different bands to individual molecular groups; alternatively, they can be seen as a characteristic fingerprint of conformational change to define or detect the transient conformational states of the protein. Similar approaches have a long history in fluorescence and absorption spectroscopy [30]. However, this is the first report on FTIR characterization of rusticyanin, so comparable information is not available at present.

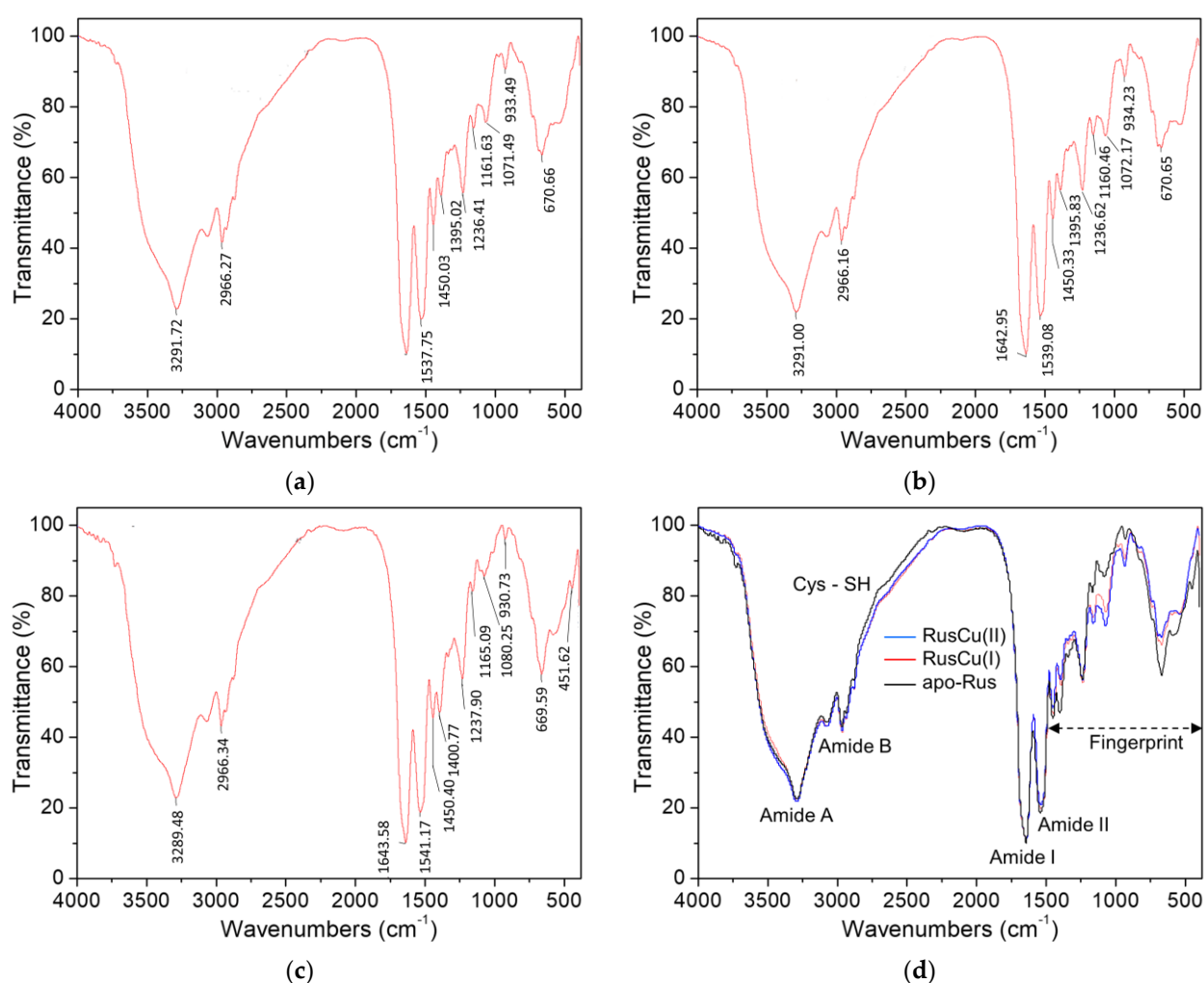
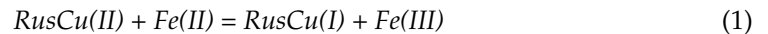


**Figure 4.** FTIR spectrum of the type-C rusticyanin from *A. ferrovorans*. (a) FTIR spectrum of the oxidized state (RusCu(I)); (b) FTIR spectrum of the reduced state (RusCu(II)); (c) FTIR spectrum of the apoprotein (apo-Rus); (d) FTIR spectrum of the apo-, oxidized and reduced state.

### 3.5. Electron Transfer from Ferrous Ion to the Type-C

Rusticyanin has been found to play a crucial role in the ferrous oxidation of *A. ferrooxidans* and was once proposed as the initial electron acceptor from ferrous ions [4,5], so the reduction in the type-C rusticyanin by ferrous ions was investigated. The one-electron-transfer reaction between the rusticyanin and iron ions is expressed using Equation (1),

where  $RusCu(II)$  represents the oxidized rusticyanin and  $RusCu(I)$  represents the reduced rusticyanin.



The kinetics for the reduction in the oxidized rusticyanin by ferrous ion to make the reduced rusticyanin can be expressed as Equation (2), where  $[RusCu(II)]$  is the concentration of the oxidized rusticyanin,  $[Fe(II)]$  is the concentration of ferrous ion, and  $k_{2nd}$  is the forward second-order reaction rate constant.

$$-d[RusCu(II)]/dt = k_{2nd} \times [Fe(II)] \times [RusCu(II)] \quad (2)$$

To obtain the second-order rate constant  $k_{on}$ , the pseudo-first-order reaction method was adopted [14]. The concentrations of iron ions were kept in 10-fold or greater excess compared to the rusticyanin concentration, ensuring pseudo-first-order conditions and thus allowing the concentration of iron ions to be treated as constant during the experiment. Then, Equation (2) can be simplified into Equation (3), in which  $k_{1st}$  is equal to the second-order rate constant  $k_{2nd}$  times the ferrous ions concentration (constant).

$$-d[RusCu(II)]/dt = k_{1st} \times [RusCu(II)] \quad (3)$$

According to the above UV-visible spectra results, the absorbance at 600 nm of the oxidized rusticyanin was selected as the probe to monitor the concentrations of the oxidized rusticyanin in the reaction. When the absorbance is directly proportional to  $[RusCu(II)]$ , the following solution to the differential Equation (3) can be written as Equation (4), where  $A_0$ ,  $A_t$  and  $A_\infty$  are the absorbances at time 0,  $t$  and  $\infty$ , respectively, and  $k_{1st}$  is the observed pseudo-first-order rate constant for the absorbance change.

$$(A_t - A_\infty) = (A_0 - A_\infty) \times \exp(-k_{1st} \times t) \quad (4)$$

Figure 5a shows the time course of absorbance at 600 nm in the presence of various concentrations of ferrous ions and the oxidized form of rusticyanin. Each of these traces provides a representative pseudo-first-order behavior of exponential decay in visual observation. When Equation (4) was fitted to each trace independently, all the theoretical lines fit the data closely, and then the pseudo-first-order rate constants for different concentrations of ferrous ion were obtained. Figure 5b shows the dependence of the pseudo-first-order rate constant for the reduction in rusticyanin by ferrous ions. The pseudo-first-order rate constants determined via linear fitting above are plotted vs. the concentrations of iron ions, where a good linear relationship between them is exhibited.

The time courses of the oxidized type-C rusticyanin reduced by various concentrations of ferrous ions all exhibited a clear pseudo-first-order kinetic exponential decay behavior with a fit R-square >99% (Figure 5a). The dependence of the pseudo-first-order rate constants upon the addition of different ferrous concentrations was highly linear; the determined second-order rate constant was about  $1.34 \text{ M}^{-1} \text{ s}^{-1}$  (Figure 5b). It was reported that the speed of the type-A rusticyanin from *A. ferrooxidans* ATCC 23270 reduced by ferrous ion was faster than that of the type-B rusticyanin from *A. ferrooxidans* JCM 3865; the second-order rate constants by ferrous reduction in the same solution conditions of HCl pH 2.0 and 100 mM NaCl at 25 °C were  $0.12 \text{ M}^{-1} \text{ s}^{-1}$  for type-A and  $0.08 \text{ M}^{-1} \text{ s}^{-1}$  for type-B [14]. Therefore, the one-electron transfer reaction from the ferrous ion to the type-C rusticyanin is obviously faster than that to both the type-A and the type-B rusticyanins. Rusticyanin has been found to play a crucial role in the ferrous oxidation of *A. ferrooxidans* and was once proposed as the initial electron acceptor from ferrous ions [4,5], so the type-C rusticyanin in the psychrotolerant *A. ferrivorans* may perform the role of initial electron receptor, which facilitates a high efficient energy gain so as to satisfy the higher energy demand of this bacterium to deal with cold growth environment conditions.

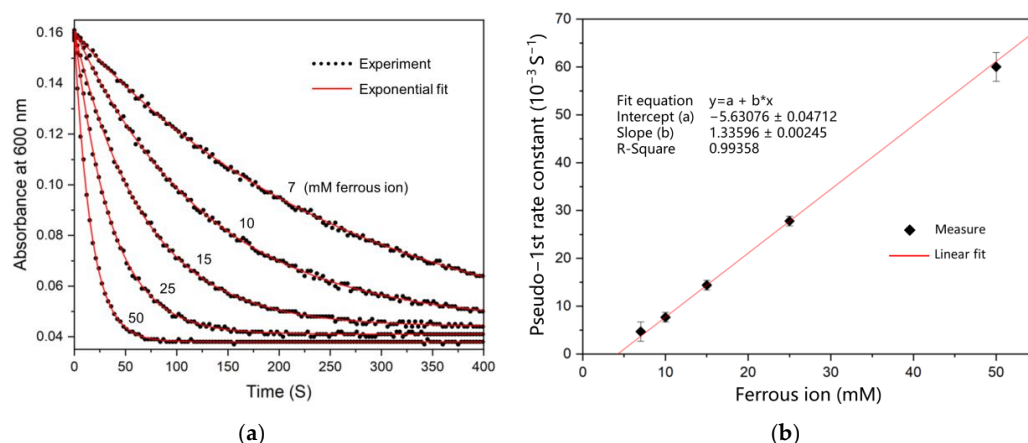


**Figure 5.** Determination of the kinetic rate constant for electron transfer from ferrous ion to the type-C from *A. ferrivorans*. (a) Time course of the absorbance changes at 600 nm when the oxidized type-C was mixed with different concentrations of ferrous ions. All reactions were maintained in the same solution conditions of HCl pH 2.0, 100 mM NaCl at 25 °C. The initial concentrations in the reaction system after mixing were as follows: the oxidized type-C rusticyanin, 0.25 mM and ferrous the ion, 7, 10, 15, 25, and 50 mM, respectively. The pseudo-first-order rate constants for different concentrations of ferrous ions were given by the exponent of the best exponential fit to each trace data. The experimental data are shown as dotted, and the theoretical fits are shown as solid lines; (b) dependence of the pseudo-first-order rate constant for the reduction in rusticyanin by ferrous ions. The pseudo-first-order rate constants determined with exponential fitting in (a) are plotted vs. the concentrations of ferrous ions. The second-order rate constants are given by the slopes of the best fit lines of linear regression. Each error bar represents the standard deviation of at least three measurements. The detailed procedure is provided in the Supplementary Material.

### 3.6. Bioinformatics Comparison of the Rusticyanins

To further reveal the essential reasons for the differences in properties between the type-C rusticyanin and other rusticyanins, a series of bioinformatics analyses were performed (Figure S1 and Table S1). The mature type-C rusticyanin from *A. ferrivorans* SS3 shares 90.32% identities and owns 15 different amino acid residues resulting in a total increase of 11.5 hydrophobicity and no change in net charge at pH 2.0 to the mature type-A from *A. ferrooxidans* ATCC 23270. The mature type-C rusticyanin also shares 92.26% identities and owns 12 different amino acid residues, resulting in a total loss of 19.2 hydrophobicity and an addition of 1 net charge at pH 2.0 to the mature type-B rusticyanin from *A. ferrooxidans* JCM 3865. There are a total of 21 mutant positions in the type-C rusticyanin compared to the type-A and the type-B rusticyanins, where 6 are mutated both in type-A and type-B; 9 are mutated only in type-A and present near the N-terminal sequence positions ranging from 1 to 74; 6 are mutated only in type-B and present near the C-terminal positions ranging from 87 to 130.

The molecular structure of the type-A rusticyanin from *A. ferrooxidans* has been determined very well, which revealed a cupredoxin fold with a six- and a seven-stranded  $\beta$ -sheet packed in a  $\beta$ -barrel arrangement hydrophobic core and an outside extending short helix forming a second hydrophobic core harboring the type I copper binding site, in addition to a unique N-terminal 35 residue extension lateral belt composed of a strand–helix–strand–strand motif [1,8,9]. The determined structure of the type-A rusticyanin enabled to further model the molecular structures of the type-C and the type-B rusticyanins and make comparisons among them at a three-dimensional molecular structure level (Figure 6a). Firstly, the N-terminal is completely exposed on the surface and extends outward to solution in the molecular structure. The recombinant type-C rusticyanin in this study only added an extra histag at the N-terminal compared to the type-A and the type-B rusticyanins. This tag brought no extra charge into the protein molecule when in a pH 2.0 solution; therefore, it is unlikely to obviously affect the properties of the protein. Secondly, 6 of 21 different

positions are in (F87FL) or near (I74VI, I56VI, N101VV, K103DN and V106VI) the hydrophobic core of the copper binding site. It was reported that the hydrophobic patches [31] and electrolytic interactions [32] in the patches surrounding the copper coordination sphere contribute to the acid-stability and redox potential of rusticyanin [1,9,18], and thus account for the decrease in the extinction coefficient, ERP signal, and kinetic rate constant of the type-B compared to the type-A rusticyanin [13,14]. Obviously, this explanation is also suitable for the differences between the type-C rusticyanin here and the type-A and B rusticyanins. Thirdly, the most important aspect is that 13 of the 21 different positions of the type-C rusticyanin are in (T1GA, P2TP, S6TS, S9EM, L18ML, V20EA, S23TS, E25KK and K29DK) or interact with (V59KV, D65ED, D117DS and K119KG) the lateral belt. The belt of rusticyanin is absent in the other cupredoxins but provides an extra lateral sheet contacts to shield the hydrophobic core, acting as a constraint belt [1,8,9]. Those mutant-specific interactions to the belt brought about a small increase in  $\beta$ -sheet contribution and significantly weakened the copper binding affinity, particularly the removal of the N-terminal 35-residue extension, which resulted in a significant impact on the characteristics of the protein and a loss of the copper [8]. Therefore, the different residues in the belt or those interacting with the constraint shield belt should be the most contributing factor to the alteration in the properties of the type-C rusticyanin observed in this study.

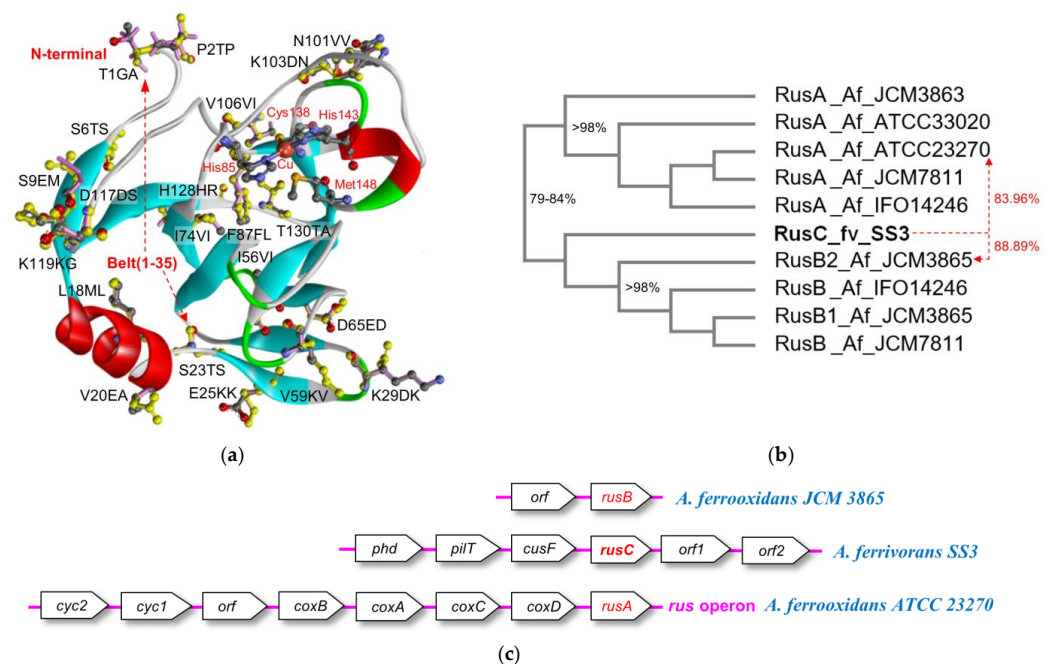


**Figure 6.** Bioinformatics analysis of the rusticyanins. (a) Molecular structure modeling of the rusticyanins and their different residues. The structure of the type-A rusticyanin from *A. ferrooxidans* ATCC 23270 (PDB: 1CUR) was taken as the template, and the molecular structures of the mature type-C rusticyanin from *A. ferrivorans* and the mature type-B rusticyanin from *A. ferrooxidans* JCM 3865 were built and superimposed together. Their different residues were displayed on the model of the type-C rusticyanin, where the residues of the type-C, type-A, and type-B rusticyanins are represented by balls and sticks in element colors, ball and stick in yellow color, and stick in purple color, respectively, and labeled with one letter and ID of type-C, one letter of type-A, and one letter of type-B for each mutant residue group. The detailed information for the different residues is referred to in Table S1; (b) phylogenetic tree of the rusticyanins from *A. ferrivorans* and various *A. ferrooxidans* sources. RusC\_fv\_SS3: the type-C rusticyanin from *A. ferrivorans* SS3; RusB2\_Af\_JCM3865: the type-B rusticyanin from *A. ferrooxidans* JCM 3865; RusA\_Af\_ATCC23270: the type-A rusticyanin from *A. ferrooxidans* ATCC 23270; other names as referred to in the sequence alignment of Figure S1; (c) gene context comparison for the genes of the type-A, type-B, and type-C rusticyanins. The detailed information is referred to in Table S2.

### 3.7. Classification of the Type-C Rusticyanin from *A. ferrivorans*

Two forms of rusticyanin have been found in various *A. ferrooxidans* strains, the more common form (type-A) was encoded by the *rus* operon and present in all studied strains till now, for instance, strain ATCC 23270; the less common form (type-B) occurred in a different gene background in some strains, for example, strain JCM 3865, and exhibited different amino acid composition, protein properties, and kinetic rate [13,14]. In contrast to the gene of type-A (*rusA*) in the *rus* operon, the gene of type-B (*rusB*) from strain JCM 3865 was reported to be situated downstream of an unknown open reading frame and with a transcriptional terminator in the 3' flanking region [13,14]. The whole genome of *A. ferrivorans* SS3 has been sequenced, and three genes (locus 0470, 1864 and 1718) of rusticyanin were also found to be present in the genome (Table S2) [17]. Sequence alignment and phylogenetic analysis for the rusticyanins from *A. ferrivorans* SS3 and various *A. ferrooxidans* were performed (Figures S1, S2 and 6b). It was reported that the type-A and type-B rusticyanins from various *A. ferrooxidans* strains had high conservation, the protein sequence identities within each form ranged from 98% to 100% and those between the different forms ranged from 79% to 80% [13,33]. The phylogenetic result here is well in line with the report on the classification of the rusticyanins from *A. ferrooxidans*. Furthermore, the gene at locus 1864 (*rusA*) from *A. ferrivorans* SS3 is situated in a gene context of the conserved *rus* operon and has a conserved amino acid sequence (nearly 92%) with the type-A rusticyanin from *A. ferrooxidans*, so it (is x) apparently corresponds to type-A. The gene at locus 1718 (*rusB*) from *A. ferrivorans* SS3 has a highly conserved amino acid sequence (near 96%) with the type-B rusticyanin from *A. ferrooxidans*, so it should correspond to type-B.

However, the gene at locus 0470 (*rusC*) from *A. ferrivorans* SS3, that encodes the protein in this study (RusC), exhibits a distinctly different sequence from both type-A and type-B of rusticyanins previously reported from *A. ferrooxidans*. Both type-A (RusA) and type-B (RusB) rusticyanins from various *A. ferrooxidans* strains are clustered into an obvious close branch in the phylogenetic tree, where the RusC from *A. ferrivorans* SS3 is slightly near (to x) the RusB branch of *A. ferrooxidans* and far from the RusA branch of *A. ferrooxidans*. The identities between the RusC from *A. ferrivorans* SS3 and the RusB branch of *A. ferrooxidans* are obviously lower than those identities higher than 98% within each branch of *A. ferrooxidans*, for example, the RusC from *A. ferrivorans* SS3 only shares 88.89% identities with the RusB from *A. ferrooxidans* JCM 3865, and 83.96% identities with the RusA from *A. ferrooxidans* ATCC 23270, respectively (Figure 6b). Similarity search in NCBI and other sequence databases for the RusC from *A. ferrivorans* SS3 were also performed, and results showed that two unclassified rusticyanins from *A. ferrivorans* (Accession WP\_071182953) and mine drainage metagenome (Accession CBI07416) has the most sequence similarity of 98.41%, while other rusticyanins from various sources were all lower than 92%. Therefore, it is difficult to classify the RusC from *A. ferrivorans* SS3 into the type-B rusticyanin, let alone the type-A rusticyanin.

Nevertheless, the gene at locus 0470 (*rusC*) from *A. ferrivorans* SS3 in this study exhibits a totally different gene context compared to those of both the *rusA* and the *rusB* (Figure 6c). The genes on the upstream of the *rusC* are *cusF* (periplasmic copper binding protein of heavy metal efflux system), *pilT* (PilT domain-containing protein) and *phd* (prevent-host-death family protein) in order; the genes on the downstream are two *orf* (hypothetical protein) (Table S2).

Then, combining the differences of the rusticyanin (RusC) from *A. ferrivorans* SS3 in protein properties, kinetic rate, sequence similarity, molecular structure, and genetic background revealed in this study to the previously reported types A and B, we tentatively propose it as a new isoform, type-C rusticyanin. The existence of this new isoform rusticyanin with high ferrous oxidation efficiency in the psychrophilic *A. ferrivorans* may satisfy the higher energy demand to deal with cold growth conditions, which is rightly in line with the previous viewpoint that rusticyanins, which are not encoded by *rus* operon, in *A. ferrivorans* may be considered as mechanisms for adaptation to low temperatures [15,16].

#### 4. Conclusions

The rusticyanin encoded by the gene at locus 0470 from the psychrophilic *A. ferrivorans* SS3 was gene-cloned, expressed, purified, and assembled in vitro. The protein exhibits extreme acid stability even at a pH of 0.3. The stability of the protein is obviously enhanced after binding of the copper cofactor, and the oxidation state is more stable than the reduced state. The protein has characteristic UV-vis peaks and EPR signals similar to the previously reported rusticyanins, but is different with a small position shift and an obvious intensity change. The vibrational spectrum of the apoprotein was more different than these between the oxidized and reduced states of the protein. The ferrous oxidation kinetic rate constant of the protein is obviously faster than that of both the type-A and type-B rusticyanins previously reported. Further bioinformatics analysis reveals their changes in sequence and molecule: the mutations related to the peculiar shield belt mostly account for the variation in the properties of the protein. The existence of the new isoform with high ferrous oxidation efficiency may facilitate the growth of the psychrophile in cold environments. So far, this is the first report on the expression and characterization of rusticyanin from the psychrotolerant *A. ferrivorans*.

**Supplementary Materials:** The following supporting information can be downloaded at: <https://www.mdpi.com/article/10.3390/separations10080448/s1>, Text S1: The specific primers used as a template for PCR amplification of the sequence area containing the type-C rusticyanin gene; Figure S1: Sequence alignment of rusticyanins from *A. ferrivorans* SS3 and various *A. ferrooxidans* sources; Figure S2: Phylogenetic tree of the rusticyanins from *A. ferrivorans* SS3 and various *A. ferrooxidans* sources according to Figure S1; Table S1: The different residues and their property differences for the type-C rusticyanin from *A. ferrivorans* SS3 compared to the type-A rusticyanin from *A. ferrooxidans* ATCC 23270 and the type-B rusticyanin from *A. ferrooxidans* JCM 3865, respectively; Table S2: Gene contexts of the rusticyanin genes in *A. ferrivorans* [17] and *A. ferrooxidans*.

**Author Contributions:** Conceptualization, Y.L.; methodology, L.C., X.S., J.H. and J.O.; software, Y.L., L.C. and X.S.; validation, R.Y., W.Z. and L.S.; formal analysis, L.C., X.S., J.O. and J.H.; investigation, L.C. and X.S.; resources, Y.L., G.Q. and X.W.; data curation, L.C., K.W., X.S. and Y.T.; writing—original draft preparation, Y.L., X.S. and L.C.; writing—review and editing, Y.L., X.S. and L.C.; visualization, L.C. and X.S.; supervision, Y.L.; project administration, Y.L.; funding acquisition, Y.L., W.Z. and G.Q. All authors have read and agreed to the published version of the manuscript.

**Funding:** This research was funded by the Changsha Municipal Natural Science Foundation (No. kq2202084), Hunan Provincial Natural Science Foundation of China (No. 2019JJ40367, No. 2015JJ2186, No. 2021JJ30855, No. 2021JJ30836), National Natural Science Foundation of China (No. 51274268, No. 50904080, No. 51934009, No. 52074353), China Postdoctoral Science Foundation (No. 2013M540643, No. 2014T70791) and National Key Research and Development Program of China (No. 2019YFC1803600). We are also grateful for resources from the High Performance Computing Center of Central South University.

**Institutional Review Board Statement:** Not applicable.

**Informed Consent Statement:** Not applicable.

**Data Availability Statement:** The data presented in this study are available on request from the corresponding author.

**Conflicts of Interest:** The authors declare no conflict of interest.

#### References

1. Botuyan, M.V.; Toy-Palmer, A.; Chung, J.; Blake, R.C., 2nd; Beroza, P.; Case, D.A.; Dyson, H.J. NMR solution structure of Cu(I) rusticyanin from *Thiobacillus ferrooxidans*: Structural basis for the extreme acid stability and redox potential. *J. Mol. Biol.* **1996**, *263*, 752–767. [[CrossRef](#)] [[PubMed](#)]
2. Valdes, J.; Pedroso, I.; Quatrini, R.; Dodson, R.J.; Tettelin, H.; Blake, R., II; Eisen, J.A.; Holmes, D.S. *Acidithiobacillus ferrooxidans* metabolism: From genome sequence to industrial applications. *BMC Genom.* **2008**, *9*, 597. [[CrossRef](#)] [[PubMed](#)]

3. Wheaton, G.; Counts, J.; Mukherjee, A.; Kruh, J.; Kelly, R. The Confluence of Heavy Metal Biooxidation and Heavy Metal Resistance: Implications for Bioleaching by Extreme Thermoacidophiles. *Minerals* **2015**, *5*, 397–451. [[CrossRef](#)]
4. Cox, J.C.; Boxer, D.H. The purification and some properties of rusticyanin, a blue copper protein involved in iron(II) oxidation from *Thiobacillus ferrooxidans*. *Biochem. J.* **1978**, *174*, 497–502. [[CrossRef](#)]
5. Ronk, M.; Shively, J.E.; Shute, E.A.; Blake, R.C., 2nd. Amino acid sequence of the blue copper protein rusticyanin from *Thiobacillus ferrooxidans*. *Biochemistry* **1991**, *30*, 9435–9442. [[CrossRef](#)]
6. Yarzabal, A.; Appia-Ayme, C.; Ratouchniak, J.; Bonnefoy, V. Regulation of the expression of the *Acidithiobacillus ferrooxidans* rus operon encoding two cytochromes c, a cytochrome oxidase and rusticyanin. *Microbiology* **2004**, *150*, 2113–2123. [[CrossRef](#)]
7. Nunzi, F.; Guerlesquin, F.; Shepard, W.; Guigliarelli, B.; Bruschi, M. Active site geometry in the high oxido-reduction potential rusticyanin from *Thiobacillus ferrooxidans*. *Biochem. Biophys. Res. Commun.* **1994**, *203*, 1655–1662. [[CrossRef](#)]
8. Grossmann, J.G. The N-terminal extension of rusticyanin is not responsible for its acid stability. *Biochemistry* **2002**, *41*, 3619. [[CrossRef](#)]
9. Barrett, M.L. Atomic resolution crystal structures, EXAFS, and quantum chemical studies of rusticyanin and its two mutants provide insight into its unusual properties. *Biochemistry* **2006**, *45*, 2939. [[CrossRef](#)]
10. Yamada, T.; Hiraoka, Y.; Das Gupta, T.K.; Chakrabarty, A.M. Rusticyanin, a bacterial electron transfer protein, causes G(1) arrest in J774 and apoptosis in human cancer cells. *Cell Cycle* **2004**, *3*, 1182–1187. [[CrossRef](#)]
11. Cruz-Gallardo, I.; Diaz-Moreno, I.; Diaz-Quintana, A.; Donaire, A.; Velazquez-Campoy, A.; Curd, R.D.; Rangachari, K.; Birdsall, B.; Ramos, A.; Holder, A.A.; et al. Antimalarial Activity of Cupredoxins the Interaction of Plasmodium Merozoite Surface Protein 1(19) (MSP1(19)) and Rusticyanin. *J. Biol. Chem.* **2013**, *288*, 20896–20907. [[CrossRef](#)] [[PubMed](#)]
12. Gonzalez-Arribas, E.; Falk, M.; Aleksejeva, O.; Bushnev, S.; Sebastian, P.; Feliu, J.M.; Shleev, S. A conventional symmetric biosupercapacitor based on rusticyanin modified gold electrodes. *J. Electroanal. Chem.* **2018**, *816*, 253–258. [[CrossRef](#)]
13. Sasaki, K. Respiratory isozyme, two types of rusticyanin of *Acidithiobacillus ferrooxidans*. *Biosci. Biotechnol. Biochem.* **2003**, *67*, 1047. [[CrossRef](#)] [[PubMed](#)]
14. Ida, C. Kinetic rate constant for electron transfer between ferrous ions and novel Rusticyanin isoform in *Acidithiobacillus ferrooxidans*. *J. Biosci. Bioeng.* **2003**, *95*, 537. [[CrossRef](#)]
15. Hedrich, S.; Schloemann, M.; Johnson, D.B. The iron-oxidizing proteobacteria. *Microbiology* **2011**, *157*, 1551–1564. [[CrossRef](#)]
16. Corahua-Santo, R.; Eca, A.; Abanto, M.; Guerra, G.; Ramirez, P. Physiological and comparative genomic analysis of *Acidithiobacillus ferrivorans* PQ33 provides psychrotolerant fitness evidence for oxidation at low temperature. *Res. Microbiol.* **2017**, *168*, 482–492. [[CrossRef](#)]
17. Liljeqvist, M.; Valdes, J.; Holmes, D.S.; Dopson, M. Draft Genome of the Psychrotolerant Acidophile *Acidithiobacillus ferrivorans* SS3. *J. Bacteriol.* **2011**, *193*, 4304–4305. [[CrossRef](#)]
18. Jafarpour, R.; Fatemi, F.; Eidi, A.; Mehrnejad, F. Effect of the Met148Leu mutation on the structure and dynamics of the rusticyanin protein from *Acidithiobacillus* sp. FJ2. *J. Biomol. Struct. Dyn.* **2021**, *39*, 4122–4132. [[CrossRef](#)]
19. Panyushkina, A.E.; Babenko, V.V.; Nikitina, A.S.; Selezneva, O.V.; Tsaplina, I.A.; Letarova, M.A.; Kostryukova, E.S.; Letarov, A.V. *Sulfobacillus thermotolerans*: New insights into resistance and metabolic capacities of acidophilic chemolithotrophs. *Sci. Rep.* **2019**, *9*, 15069. [[CrossRef](#)]
20. Sousa, P.; Camacho, I.; Câmara, J.S.; Perestrello, R. Urinary Proteomic/Peptidomic Biosignature of Breast Cancer Patients Using 1D SDS-PAGE Combined with Matrix-Assisted Laser Desorption/Ionization-Time of Flight Mass Spectrometry. *Separations* **2023**, *10*, 291. [[CrossRef](#)]
21. Zeng, J.; Geng, M.; Liu, Y.; Xia, L.; Liu, J.; Qiu, G. The sulfhydryl group of Cys 138 of rusticyanin from *Acidithiobacillus ferrooxidans* is crucial for copper binding. *Biochim. Biophys. Acta-Proteins Proteom.* **2007**, *1774*, 519–525. [[CrossRef](#)] [[PubMed](#)]
22. Zeng, J.; Geng, M.; Liu, Y.; Zhao, W.; Xia, L.; Liu, J.; Qiu, G. Expression, purification and molecular modelling of the Iro protein from *Acidithiobacillus ferrooxidans* Fe-1. *Protein Expr. Purif.* **2007**, *52*, 146–152. [[CrossRef](#)] [[PubMed](#)]
23. Bowers, K.; Markova, N. Value of DSC in Characterization and Optimization of Protein Stability. In *Microcalorimetry of Biological Molecules: Methods and Protocols*; Ennifar, E., Ed.; Methods in Molecular Biology; Humana Press: New York, NY, USA, 2019; Volume 1964, pp. 33–44.
24. Wen, J.; Arthur, K.; Chemmalil, L.; Muzammil, S.; Gabrielson, J.; Jiang, Y. Applications of differential scanning calorimetry for thermal stability analysis of proteins: Qualification of DSC. *J. Pharm. Sci.* **2012**, *101*, 955–964. [[CrossRef](#)]
25. Feng, J.; Cai, H.; Wang, H.; Li, C.; Liu, S. Improved oxidative stability of fish oil emulsion by grafted ovalbumin-catechin conjugates. *Food Chem.* **2018**, *241*, 60–69. [[CrossRef](#)]
26. Brandes, N.; Welzel, P.B.; Werner, C.; Kroh, L.W. Adsorption-induced conformational changes of proteins onto ceramic particles: Differential scanning calorimetry and FTIR analysis. *J. Colloid Interface Sci.* **2006**, *299*, 56–69. [[CrossRef](#)]
27. Wu, T.; Jiang, Q.; Wu, D.; Hu, Y.; Chen, S.; Ding, T.; Ye, X.; Liu, D.; Chen, J. What is new in lysozyme research and its application in food industry? A review. *Food Chem.* **2019**, *274*, 698–709. [[CrossRef](#)]
28. Alderton, A.L.; Faustman, C.; Liebler, D.C.; Hill, D.W. Induction of redox instability of bovine myoglobin by adduction with 4-hydroxy-2-nonenal. *Biochemistry* **2003**, *42*, 4398–4405. [[CrossRef](#)] [[PubMed](#)]
29. Sartor, G.; Mayer, E.; Johari, G.P. Calorimetric studies of the kinetic unfreezing of molecular motions in hydrated lysozyme, hemoglobin, and myoglobin. *Biophys. J.* **1994**, *66*, 249–258. [[CrossRef](#)] [[PubMed](#)]

30. Barth, A.; Zscherp, C. What vibrations tell us about proteins. *Q. Rev. Biophys.* **2002**, *35*, 369–430. [[CrossRef](#)]
31. Kyte, J.; Doolittle, R.F. A simple method for displaying the hydropathic character of a protein. *J. Mol. Biol.* **1982**, *157*, 105–132. [[CrossRef](#)]
32. Gutfreund, H. Proteins: Structures and molecular properties (second edition). *FEBS Lett.* **1993**, *323*, 294. [[CrossRef](#)]
33. Ida, C.; Sasaki, K.; Ohmura, N.; Ando, A.; Saiki, H. Classification of rusticyanin structure genes from five different strains of *Thiobacillus ferrooxidans* into two groups. *Process Metall.* **1999**, *9*, 129–137. [[CrossRef](#)]

**Disclaimer/Publisher’s Note:** The statements, opinions and data contained in all publications are solely those of the individual author(s) and contributor(s) and not of MDPI and/or the editor(s). MDPI and/or the editor(s) disclaim responsibility for any injury to people or property resulting from any ideas, methods, instructions or products referred to in the content.